Electronic Supplementary Material (ESI) for Physical Chemistry Chemical Physics.

Supporting information

What accounts for the different functions in Photolyases and Cryptochromes: a computational study of proton transfers to FAD

Daniel Holub,[a] Tomáš Kubař, [a] Thilo Mast,[a] Marcus Elstner, [ab] and Natacha Gillet[ac]

[a] *Department for Theoretical Chemical Biology, Institute for Physical Chemistry, Karlsruhe Institute for Technology, Kaiserstr. 12, 76131, Karlsruhe, Germany.*

[b] *Institute of Biological Interfaces (IGB2), Karlsruhe Institute for Technology, Kaiserstr. 12, 76131, Karlsruhe, Germany*

[c] *Institut de Génétique et de Biologie Moléculaire et Cellulaire (IGBMC), Institut National de La Santé et de La Recherche Médicale (INSERM), U1258/Centre National de Recherche Scientifique (CNRS), UMR7104/Université de Strasbourg, 67404 Illkirch, France.*

E-mail: natacha.gillet@kit.edu

I. Structural reorientations triggered by the $FAD^{\bullet-}$ formation in MD

PL-WT

Two main structural changes are observed in MD simulation with $FAD^{\bullet-}$: the rotation of the Asn378, illustrated by the distance fluctuations between the side chain Asn378 nitrogen atom (Figure S1) and the presence of water molecules in the FAD pocket (Figure S2).

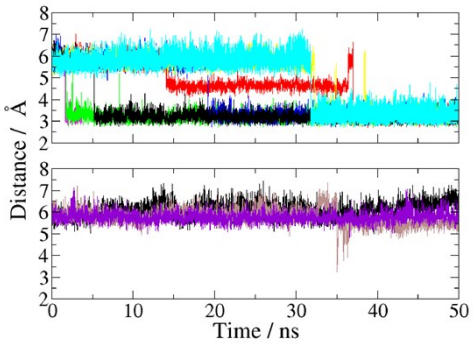

Figure S1: Distance between the side chain of Asn378 nitrogen and N5 of FAD in the 10 individual MD simulations. Top: seven runs with starting O-conformation and final N-conformation. Bottom: three simulations with stable O-conformation.

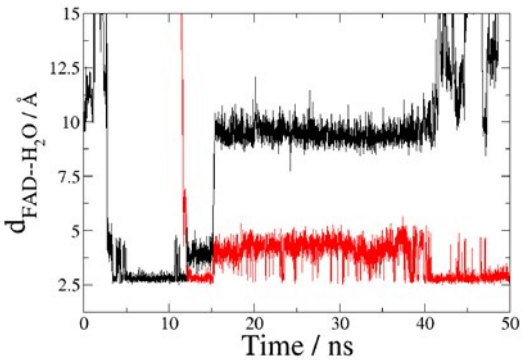

Figure S2: Distance between the centre of mass of water molecules which come inside the FAD pocket and FAD N5. Distances of less than 3 Å indicate that the water is in the FAD pocket.

PL-N378D and CRYI

In CRYI, the distan*ce* between the proton of Asp396 and the FAD N_5 is on average smaller than in PL-N378D, where on the contrary the distance between the O_4 of FAD and the proton is smaller. Indeed, the proton of Asp396 in CRYI faces more often the N_5 of FAD than in PL-N378D. The neighbouring amino acids (Arg344-Asp372 in PL-N378D, Arg362-Asp390 in CRYI) show a conserved salt bridge and the relative positions of Arg344/362 and FAD slightly differ in the two proteins (**Table S1** and **Figure S3**). A further difference is seen in the standard deviations of the distances between the proton of the Asp and the Arg-Asp salt bridge, which are larger in CRYI, indicating a higher structural flexibility.

Table S1: Averaged distances and corresponding standard deviations along the 200 ns trajectory including the $FAD^{\bullet-}$ state after a 100 ns simulation with neutral FAD in PL-N378D and CRYI. The numbering of Asp374, Asp372 and Asp378 corresponds in CRYI to Asp392, Asp390 and Asp396.

	PL-N378D Distance / Å	CRYI Distance / Å
FAD N_5 - Arg C_ζ	4.42 ± 0.23	4.86 ± 0.77
Arg C_ζ - Asp372	3.98 ± 0.10	4.16 ± 0.30
FAD O_4 - Asp374	2.25 ± 0.28	3.00 ± 0.18
FAD O_4 - Asp378	1.91 ±0.54	1.99 ± 0.46
FAD N_5 - Asp378	2.79 ± 0.52	2.64 ± 0.40

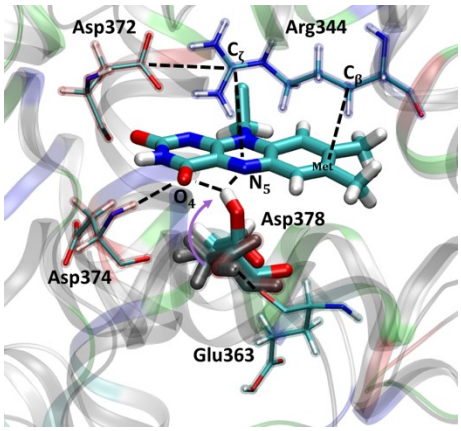

Figure S3: overlap of the FAD binding pocket for FAD_{ox} (grey) and $FAD^{\bullet-}$ (colour) states. The purple arrow indicates the rotation of Asp378/396. Dashed lines refer to the distances listed in Table S1. The numbering of Asp374, Asp372, Asp378, Arg344 and Glu363 corresponds to PL-N378D and to the respective homologs Asp392, Asp390, Asp396, Arg362 and Met381 in CRYI.

II. Structural reorientations triggered by the $FAD^{\bullet-}$ formation: free energies

Rotation of Asn378

Table S2: Calculated barrier heights of the rotation of χ in Asn378 for FAD_{ox} and $FAD^{\bullet-}$ and the corresponding reaction constants

	$Barrier_{O\text{-}N\text{-}conformation}$ (kcal·mol^{-1})	$Barrier_{N\text{-}O\text{-}conformation}$ (kcal·mol^{-1})	$k_{O\text{-}N}$ (ns^{-1})	$k_{\text{-}O\text{-}N}$ (ns^{-1})	K_{eq}
FAD	8.14	4.67	0.007	2.48	0.0028
$FAD^{\bullet-}$	2.31	6.12	130	0.22	590

Formation of a water wire

To study the free energy for the formation of the water wire we constrained the Asn378 in the O-conformation to avoid sampling issues with regards to the Asn378 rotation. We randomly selected a water, located in the exterior of the pocket at about 6 Å from the FAD N_5 and used this distance as reaction coordinate for US. The formation of a water wire would require another water molecule to enter, so, we used the distance between the first water molecule, now constrained in the pocket, 3 Å away from FAD N_5, and a water molecule from the bulk.

Taken together, the barrier height for the entrance of the first water molecule is probably underestimated because the rotation from the N-conformation to the O-conformation, which competes with the entrance of water in the pocket, cannot occur in the US simulations. Additionally, the barrier height for the entrance of the second water molecule might be overestimated because (I) the first water is partially constrained in the simulations, (II) the second water was not allowed to penetrate deeper into the pocket; the interaction between the two water molecules might thus be underestimated.

III. Electrostatic interaction in the FAD pocket

Table S3: Averaged E_{Coul} values (in kcal·mol^{-1}) between solvent, protein, side chain of Asp378/396 and FAD ISO for the FAD$^{\bullet -}$-AspH or FADH$^{\bullet}$-Asp^{-} states.

Coulomb energy in kcal·mol^{-1}		**Adduct FAD^{-}-ASP-H** E_{Coul}(adduct)		**Product FADH-ASP^{-}** E_{Coul}(product)		ΔE	
System		CRYI	PL-N378D	CRYI	PL-N378D	CRYI	PL-N378D
FAD	Solvent	-20.34	-20.98	-12.52	-12.97	7.82	8.00
ASP	Solvent	0.06	-0.04	-13.34	-0.53	-13.40	-0.49
FAD	Protein	-4.78	-8.06	-4.67	-7.21	0.11	0.85
ASP	Protein	-25.79	-35.15	-27.5	-46.16	-1.71	-11.01
FAD	ASP	-15.52	-15.17	-12.24	-11.88	3.27	3.29
sum		**-66.36**	**-79.38**	**-70.27**	**-78.75**	**-3.91**	**20.64**

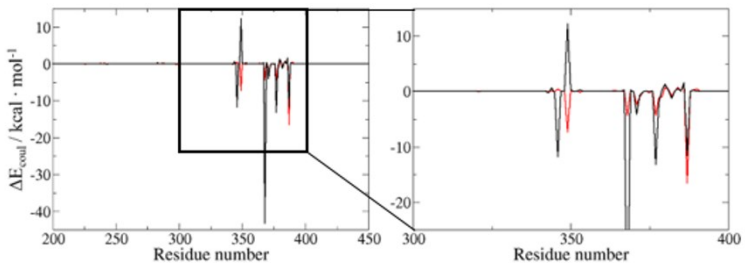

Figure S4: Electrostatic interaction difference, ΔE_{Coul}, between each side chain of the protein residues (black for PL-N378D, red for CRYI) and the the FAD$^{\bullet -}$-AspH or FADH$^{\bullet}$-Asp^{-} states. Right: zoomed in view of the important, stronger interacting residues (300-400), mostly located in the FAD pocket.

IV. Proton transfer in PL-N378D

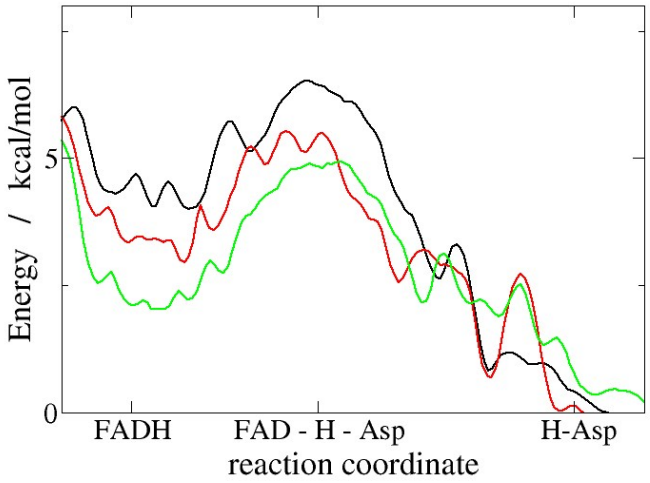

Figure S5: US QM/MM free energy landscapes of the proton transfer between Asp378 and FAD in PL-N378D for different states of amino acid Glu363 in PL-N378D: protonated (green) or deprotonated (red) curve and for the E363M mutant (black).

V. Calculated Orbital energy of FADH•

To calculate the response of the FAD pocket to the new charge state of FAD, $FADH^-$, a quantum mechanical treatment of the active site has to be included *via* a so-called combined Quantum Mechanics/Molecular Mechanics (QM/MM) scheme. The structural part of interest, the isoalloxazine ring of FAD, was calculated by QM at DFTB level[2] and the remaining atoms are treated classically using force fields (MM) and affect the QM-zone by electrostatic interactions. Hydrogen link atoms[1] are inserted at the QM/MM boundary, namely in the C1-C2 bond of the FAD D-ribitol tail.

The Energy of FAD is represented by only one frontier orbital, so, the chosen *i*-th fragment orbital (FO) of the fragment *m* is expressed in an atomic basis set χ_μ and determined by FO coefficients c_μ^i: [3,4]

$$\varphi_m^i = \sum_\mu c_\mu^i \chi_\mu \qquad (1)$$

This FO-DFTB approach has been extensively evaluated and tested in previous publications [3,5,6] and has been so far successfully applied to describe the charge transfer in photolyase,[7] cryptochrome[8] and DNA[9,10] where the HOMO's of the fragments were also used to calculate the relation between the decrease of the energy induced by the structural reorientation of the environment. We calculated the energy of $FADH^-$ using FO-DFTB/MM approach along a 400 ps simulation (Figure S6). The energetic decrease can be interpreted as the stabilization of the negatively charged state in the FAD pocket of FAD.

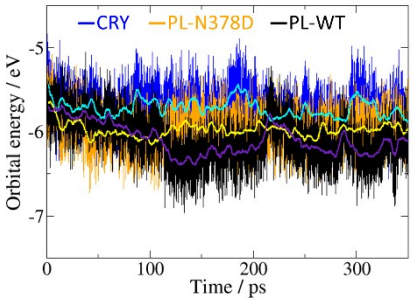

Figure S6: Orbital energy of $FADH^-$. The energy of the HOMO of $FADH^-$ is calculated in a 350 ps QM/MM MD simulation. The curves show the fluctuation of the orbital energy induced by the environment of the FAD pocket (CRY blue and averaged value cyan, orange PL-N378D and averaged value yellow and WT-PL black and averaged value purple).

1 M. J. Field, P. A. Bash and M. Karplus, *J. Comput. Chem.*, 1990, **11**, 700–733.
2 M. Elstner, D. Porezag, G. Jungnickel, J. Elsner, M. Haugk, T. Frauenheim, S. Suhai and G. Seifert, *Phys. Rev. B*, 1998, **58**, 7260.
3 T. Kubar and M. Elstner, *J. R. Soc. Interface*, 2013, **10**, 20130415–20130415.
4 A. Kubas, F. Gajdos, A. Heck, H. Oberhofer, M. Elstner and J. Blumberger, *Phys Chem Chem Phys*, 2015, **17**, 14342–14354.
5 T. Kubař and M. Elstner, *Phys. Chem. Chem. Phys.*, 2013, **15**, 5794–5813.
6 A. Heck, P. B. Woiczikowski, T. Kubař, K. Welke, T. Niehaus, B. Giese, S. Skourtis, M. Elstner and T. B. Steinbrecher, *J. Phys. Chem. B*, 2014, **118**, 4261–4272.
7 G. Lüdemann, P. B. Woiczikowski, T. Kubař, M. Elstner and T. B. Steinbrecher, *J. Phys. Chem. B*, 2013, **117**, 10769–10778.
8 G. Lüdemann, I. A. Solov'yov, T. Kubař and M. Elstner, *J. Am. Chem. Soc.*, 2015, **137**, 1147–1156.
9 T. Kubař, P. B. Woiczikowski, G. Cuniberti and M. Elstner, *J. Phys. Chem. B*, 2008, **112**, 7937–7947.
10 T. Kubař and M. Elstner, *J. Phys. Chem. B*, 2008, **112**, 8788–8798.